Fe^{2+}-Catalyzed Oxidation and Cleavage of Sarcoplasmic Reticulum ATPase Reveals Mg^{2+} and Mg^{2+}−ATP Sites†

Suming Hua and Giuseppe Inesi*

Department of Biochemistry and Molecular Biology, University of Maryland School of Medicine, Baltimore, Maryland 21201

Hiromi Nomura and Chikashi Toyoshima

Institute of Molecular and Cellular Biosciences, University of Tokyo, Bunkyo-ku, Tokyo 113, Japan

Received May 23, 2002; Revised Manuscript Received July 15, 2002

ABSTRACT: Fe^{2+} can substitute for Mg^{2+} in activation of the sarcoplasmic reticulum (SR) ATPase, permitting approximately 25% activity in the presence of Ca^{2+}. Therefore, we used Fe^{2+} to obtain information on the binding sites for Mg^{2+} and the Mg^{2+}−ATP complex within the enzyme structure. When the ATPase is incubated with Fe^{2+} in the presence of H_2O_2 and/or ascorbate, specific patterns of Fe^{2+}-catalyzed oxidation and cleavage are observed in the SR ATPase, depending on its Ca^{2+}-bound (E1-Ca_2) or Ca^{2+}-free conformation (E2-TG), as well as on the presence of ATP. The ATPase protein in the E1-Ca_2 state is cleaved efficiently by Fe^{2+} with H_2O_2 and ascorbate assistance, yielding a 70−75 kDa carboxyl end fragment. Cleavage of the ATPase protein in the E2-TG state occurs within the same region, but with a more diffuse pattern, yielding multiple fragments within the 65−85 kDa range. When Fe^{2+} catalysis is assisted by ascorbate only (in the absence of H_2O_2), cleavage at the same protein site occurs much more slowly, and is facilitated by ATP (or AMP-PNP) and Ca^{2+}. Amino acid sequencing indicates that protein cleavage occurs at and near Ser346, and is attributed to Fe^{2+} bound to a primary Mg^{2+} site near Ser346 and neighboring Glu696. In addition, incubation with Fe^{2+} and ascorbate produces Ca^{2+}- and ATP-dependent oxidation of the Thr441 side chain, as demonstrated by NaB^3H_4 incorporation and analysis of fragments obtained by extensive trypsin digestion. This oxidation is attributed to bound Fe^{2+}−ATP complex, as shown by structural modeling of the Mg^{2+}−ATP complex at the substrate site.

The Ca^{2+} transport ATPase of sarcoplasmic reticulum consists of a 997 amino acid chain, partitioned in 10 transmembrane segments (M1−M10) and a cytosolic headpiece that includes 3 discrete domains (*1*, *2*). The A domain corresponds to the N-terminal loop and that connecting the M2 and M3 helices. The P domain is formed by folding of two relatively distant segments within the loop connecting the M4 and M5 helices and is separated by the N domain. The P domain contains the residue (Asp351) undergoing phosphorylation by ATP. The N domain contains the adenosine binding pocket formed by residues including Phe487, Lys492, and Lys515. A, P, and N domains are folded to form a compact headpiece in the absence of Ca^{2+} (*2*−*4*). On the other hand, they rotate and become quite separated in the presence of Ca^{2+} (*1*). In the crystal structure of the Ca^{2+}-bound form (*1*), the adenosine binding pocket and the phosphorylation site are separated by about a 25 Å distance. Utilization of ATP therefore requires approximation of the N and P domains, so that the terminal phosphate of ATP bound to the N domain may reach Asp351 in the P domain. Acidic residues of critical importance are clustered around this residue of phosphorylation (*5*, *6*). Accordingly, an important feature of catalytic interactions is related to Mg^{2+}, as a component of the Mg^{2+}−ATP substrate complex, and also as an independent ligand required for catalytic functions in the phosphorylation by P_i. Nonetheless, its position in the ATPase remains ambiguous because the crystal structures did not show bound Mg^{2+} (*1*, *2*).

Mg^{2+} interactions with the Na^+, K^+-ATPase were recently investigated by substituting Mg^{2+} with Fe^{2+}, and determining the location of Fe^{2+}-induced peptide cleavage (*7*). In fact, diffusible hydroxyl radicals are produced by Fe^{2+} reaction with H_2O_2, or following reduction of bound iron with ascorbate, and abstract α-hydrogen atoms from the peptide backbone. The resulting carbon-centered radicals then react with O_2 and induce various cleavage reactions (*8*, *9*). Oxidation of side chains, such as that of threonine residues, can also occur in certain cases (*10*). We report here studies of the SR[1] Ca^{2+} ATPase, demonstrating specific patterns of oxidation and protein cleavage in the presence and the absence of Ca^{2+} and ATP.

† This work was supported by National Institutes of Health Program Project HL27867 and the Human Frontier Science Program.

* To whom correspondence should be addressed. Tel.: 410-706-3220; Fax: 410-706-8297; E-mail: ginesi@umaryland.edu.

[1] Abbreviations: AMP-PNP, 5′-adenylyl imidodiphosphate; DTT, DL-dithiothreitol; EGTA, ethylene glycol bis(β-aminoethyl ether)-*N*,*N*,*N*′,*N*′-tetraacetic acid; FITC, fluorescein-5-isothiocyanate; HPLC, high-performance liquid chromatography; MOPS, 4-morpholinepropanesulfonic acid; PYP, pyridoxal 5′-phosphate; SDS, sodium dodecyl sulfate; SR, sarcoplasmic reticulum; TG, Thapsigargin; TRIS, tris-(hydroxymethyl)aminomethane.

10.1021/bi026181u CCC: $22.00
Published on Web 08/28/2002

METHODS

Ca^{2+} ATPase Preparations. SR vesicles were obtained from skeletal muscle as described by Eletr and Inesi (*11*). Total protein was measured by the BCA protein assay reagent (Pierce). In this preparation, the Ca^{2+} ATPase accounts for approximately 50% of the total protein content, i.e., 4−5 nmol of ATPase/mg of total protein. *E1-Ca_2*, i.e., the ATPase state activated by Ca^{2+}, was obtained by simply placing the vesicles in a medium containing 20 mM MOPS, pH 7.0, 80 mM KCl, 15 μM Ca^{2+}, and other additions as required by the experimental schedule. *E2-TG*, i.e., the inactive ATPase stabilized by TG binding, was obtained by placing 1 mg of SR protein in 1 mL of 2 mM EGTA, 20 mM MOPS, pH 7.0, 80 mM KCl, and 20 μM TG. Following a 15 min incubation at 22 °C, this mixture was diluted 10-fold with 10 mM MOPS, pH 7.0, containing 10% sucrose (washing buffer). The vesicles were sedimented by centrifugation at 100000*g* for 35 min, and the pellet was then rinsed 3 times with washing buffer. The final pellet (approximately 0.5 mg of protein) was resuspended in 30 μL of washing buffer. This method allowed elimination of the EGTA used to chelate Ca^{2+}, and to maintain the inactive E2 state by stabilization with TG (*12*).

Derivatization of the ATPase at Lys515 with FITC, derivatization at Lys492 with pyridoxal phosphate, and mutation of Arg560 to Ala were obtained as previously described (*13*).

ATPase activity was measured by colorimetric determination of P_i production (*14*). The incubation was performed with a mixture containing 10 μg of SR protein/mL, 20 mM MOPS, pH 7.0, 80 mM KCl, 50 μM $CaCl_2$, 3.0 μM A23187 (ionophore), 0.1 mM ATP, and either 0.1 mM $MgCl_2$ or 0.1 mM $FeSO_4$. The temperature was 37 °C.

ATPase Cleavage with Fe^{2+}. In most cases, 1.0 mg of SR protein was incubated in 1.0 mL of a medium containing 20 mM MOPS, pH 7.0, 80 mM KCl, 50 μM $FeSO_4$, 5 mM ascorbate, 5 mM H_2O_2, in the absence of added Ca^{2+} (for E2-TG) or in the presence of 15 μM $CaCl_2$ (for E1-Ca_2). In some cases, the incubation was carried out in the absence of H_2O_2, or in the presence of ATP. Following 5 min (50 min, if H_2O_2 was not added) incubation at 22 °C, 20 μL of the reaction mixture was added to 10 μL of a medium containing 50 mM TRIS, pH 8.0, 1% SDS, 0.5 mM mercaptoethanol, and 1% Coomassie Blue. The solubilized sample was then loaded on 12% gels for electrophoretic separation (*15*) and staining with Coomassie Blue. Electrophoretic bands of interest (before staining) were transblotted onto Immobilon-P membranes in the presence of 0.2 mM DTT, stained with Amido Black, and submitted to amino acid sequencing.

Reduction of Oxidized Product with NaB^3H_4. After a 50 min incubation as described above (but in the absence of H_2O_2), NaB^3H_4 was added to yield a 100 μM concentration, followed by incubation for 1 h and centrifugation at 100000*g* for 35 min. The pellet was resuspended in 10 mM MOPS, pH 7, and 10% sucrose, to yield 1 mg of SR protein/mL. The sample was then digested with trypsin (1:10 SR protein) for 30 min at 37 °C, and centrifuged again at 100000*g* for 35 min. The supernatant was collected and digested with trypsin (1:50 SR protein) for 4 h at 37 °C. The soluble fragments were then separated by HPLC (0.1% trifluoroacetic acid in H_2O to acetonitrile 90% and 0.1% trifluoroacetic acid). The radioactive fraction obtained from the first HPLC separation was passed again through the HPLC column (10 mM ammonium acetate in H_2O to 10 mM ammonium acetate in 90% acetonitrile). A single radioactive peptide eluted from this second column was then submitted to amino acid sequencing, and the product of each Edman degradation cycle was collected for measurement of ^{3}H-radioactivity.

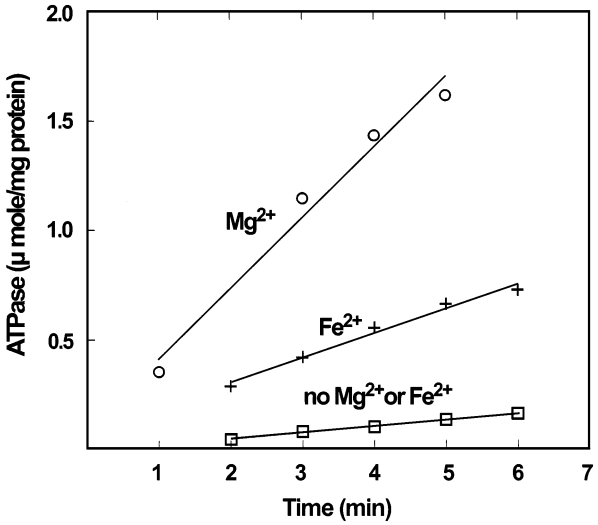

FIGURE 1: Activation of Ca^{2+}-dependent ATPase activity by Mg^{2+} or Fe^{2+}. ATPase activity was measured by colorimetric determination of P_i production (*14*). The incubation was performed with a mixture containing 10 μg of SR protein/mL, 20 mM MOPS, pH 7.0, 80 mM KCl, 50 μM $CaCl_2$, 3.0 μM A23187 (ionophore), 0.1 mM ATP, and either 0.1 mM $MgCl_2$ or 0.1 mM $FeSO_4$. The temperature was 37 °C.

RESULTS

Effect of Fe^{2+} on ATPase Activity. Mg^{2+} is a strict requirement for SR ATPase activity in the presence of Ca^{2+}. It is shown in Figure 1 that Fe^{2+} can substitute for Mg^{2+}, yielding approximately 25% of the ATPase activity observed in the presence of Mg^{2+}. Therefore, we utilized Fe^{2+} (as a substitute for Mg^{2+}) to produce oxidation and protein cleavage with the assistance of H_2O_2 and/or ascorbate, and to obtain information on the binding sites for Mg^{2+} and the Mg^{2+}−ATP complex, based on the location of Fe^{2+}-induced oxidation and cleavage within the protein structure.

Characterization of Cleavage Products. We performed an initial group of experiments to characterize the cleavage of Ca^{2+} ATPase by Fe^{2+} with the assistance of H_2O_2 and ascorbate, as done by Patchornik et al. (*7*) with the Na^+, K^+ ATPase. A set of samples was incubated in the presence of Ca^{2+}, to obtain the E1-Ca_2 conformation. Another set of samples contained ATPase in the E2-TG conformation (see Methods) and was incubated in the absence of added Ca^{2+}.

Cleavage of the enzyme occurred quite efficiently within 5 min incubation of E1-Ca_2 with Fe^{2+} in the presence of H_2O_2 and ascorbate, as shown by decreased intensity of the 100 kDa ATPase band on electrophoresis, and appearance of a 70−75 kDa band (Figure 2). On the other hand, incubation of E2-TG in the absence of Ca^{2+} produced several bands within the 65−85 kDa range (Figure 2). The cleavage patterns of E1-Ca_2 or E2-TG were not significantly influenced by ATP (Figure 2). We concluded that, under these

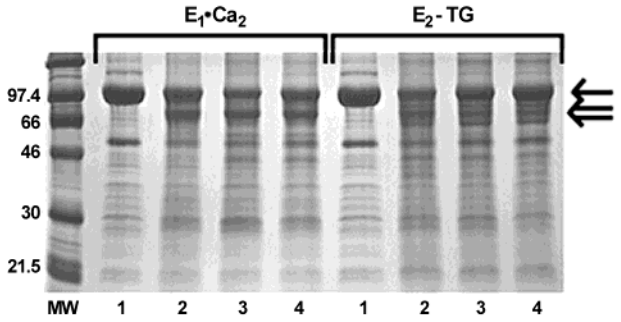

FIGURE 2: Patterns of ATPase protein cleavage following incubation with Fe^{2+}, ascorbate, and H_2O_2. Incubation with Fe^{2+}, ascorbate, and H_2O_2 for 5 min, solubilization, and electrophoresis were performed as described under Methods. A set of samples was incubated in the presence of Ca^{2+} (E1-Ca_2), and another set in the absence of Ca^{2+} (E2-TG). 1, control; 2, no ATP or Mg^{2+}; 3, 0.2 mM ATP; 4, 0.2 mM ATP and 5 mM $MgCl_2$. The single arrow indicates the ATPase band, and the double arrow indicates cleavage products. The MW numbers refer to kDa.

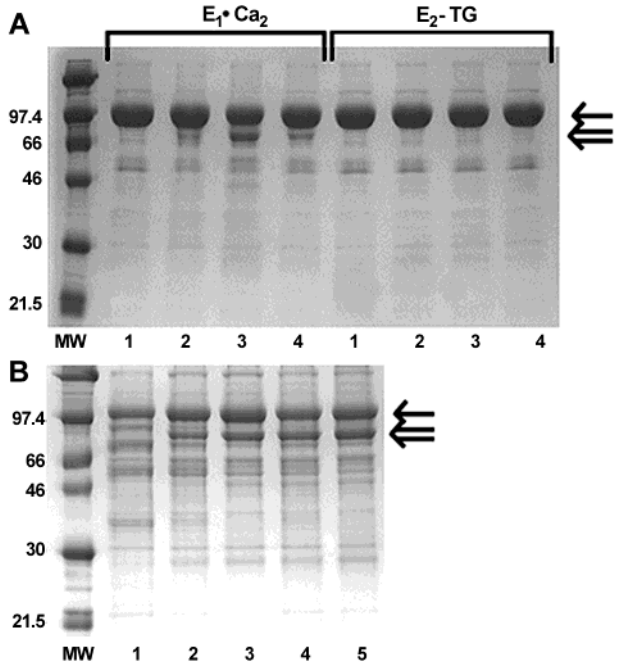

FIGURE 3: Patterns of ATPase protein cleavage following incubation with Fe^{2+} and ascorbate. Incubation with Fe^{2+} and ascorbate, solubilization, and electrophoresis were performed as described under Methods. (A) A set of samples was incubated for 50 min in the presence of Ca^{2+} (E1-Ca_2), and another set in the absence of Ca^{2+} (E2-TG). 1, control; 2, no ATP or Mg^{2+}; 3, 0.2 mM ATP; 4, 0.2 mM ATP and 5 mM $MgCl_2$. (B) Incubation of E1-Ca_2 with Fe^{2+} and ascorbate in the presence of 0.2 mM ATP was carried out for 0, 15, 30, 60, and 180 min (lanes 1−5).The single arrow indicates the ATPase band, and the double arrow indicates cleavage products. The MW numbers refer to kDa.

conditions, Fe^{2+} may bind directly to the Ca^{2+} ATPase, and the resulting cleavage is more localized when the enzyme is in the E1-Ca_2 state than in the E2-TG state.

In another group of experiments, we used ascorbate only, in the absence of H_2O_2, to assist the Fe^{2+} reaction. In this case, cleavage proceeded much more slowly, and a 3 h incubation was required to obtain a well-evident 70−75 kDa cleavage band (Figure 3). Under these conditions, cleavage was facilitated by Ca^{2+} and ATP, and was inhibited by Mg^{2+}. No significant cleavage was obtained if E2-TG, rather than E1-Ca_2, was used (Figure 3). We found that catalytic

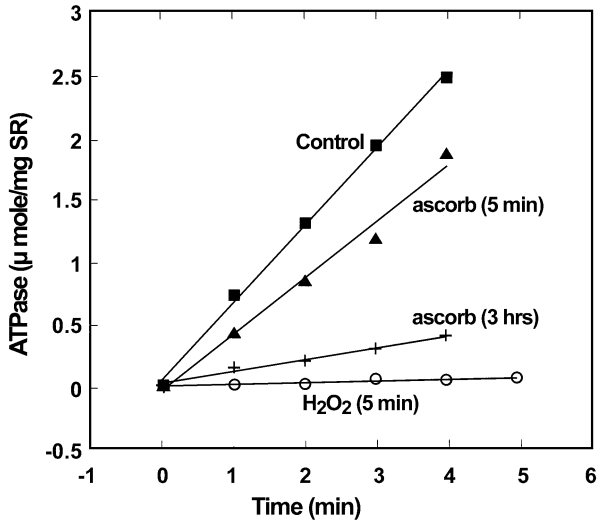

FIGURE 4: Effects of preincubation with Fe^{2+} in the absence or in the presence of ascorbate or H_2O_2 on Ca^{2+}-dependent ATPase activity. Preincubations with 0.1 mM $FeSO_4$, in the absence or in the presence of 5 mM H_2O_2 or 5 mM ascorbate, were carried out as described under Methods. ATPase activity was measured by colorimetric determination of P_i production (*14*). The incubation was performed with a mixture containing 10 μg of SR protein/mL, 20 mM MOPS, pH 7.0, 80 mM KCl, 50 μM $CaCl_2$, 3.0 μM A23187 (ionophore), 0.1 mM ATP, and either 0.1 mM $MgCl_2$ or 0.1 mM $FeSO_4$. The temperature was 37 °C.

inactivation occurs in parallel with protein cleavage, i.e., fast with the assistance of H_2O_2 and more slowly with the assistance of ascorbate only (Figure 4).

In the presence of Ca^{2+}, half-maximal activation of cleavage was obtained with 50 μM ATP or AMP-PNP, while addition of nucleotide at concentrations higher than that of Fe^{2+} was inhibitory (Figure 5). If the ATPase was derivatized with FITC at Lys515 or with PYP at Lys492, or Arg560 mutated to Ala, to interfere with ATP binding (*16*), no cleavage by Fe^{2+} was observed (not shown). Mutation of Glu771 to Gln, which interferes with Ca^{2+} binding and enzyme activation (*17*), also interfered with the ATP-dependent cleavage by Fe^{2+} (not shown). In the presence of AMP-PNP, Mg^{2+} inhibited the ATPase cleavage by Fe^{2+}, producing half-maximal inhibition at approximately 0.2 mM concentration (Figure 6). It is then apparent that the slow ATPase cleavage obtained in the presence of Fe^{2+} and ascorbate (H_2O_2 absent) can be detected only when the enzyme resides in the conformational state produced by Ca^{2+} and ATP binding.

Amino acid sequencing of the 70−75 kDa band obtained in the presence of Ca^{2+} and ATP yielded a sequence attributed to ^{346}SVICS, and consistent with the 70−75 kDa size of the fragment. Edman degradation, however, yielded a rather weak signal and more than a single amino acid per cycle. This suggests that cleavage by Fe^{2+} was not exclusively at Ser346, but involved to some extent neighboring residues, resulting in considerable heterogeneity of the amino-terminal end of the peptide fragment. It is also possible that a fraction of the cleavage product resulted in N-terminal blockage (*9*).

Characterization of Oxidation Products. We considered that in some cases Fe^{2+} binding may cause oxidation that does not result in the cleavage of peptide bonds, and that separate experiments are needed to detect them. To this aim,

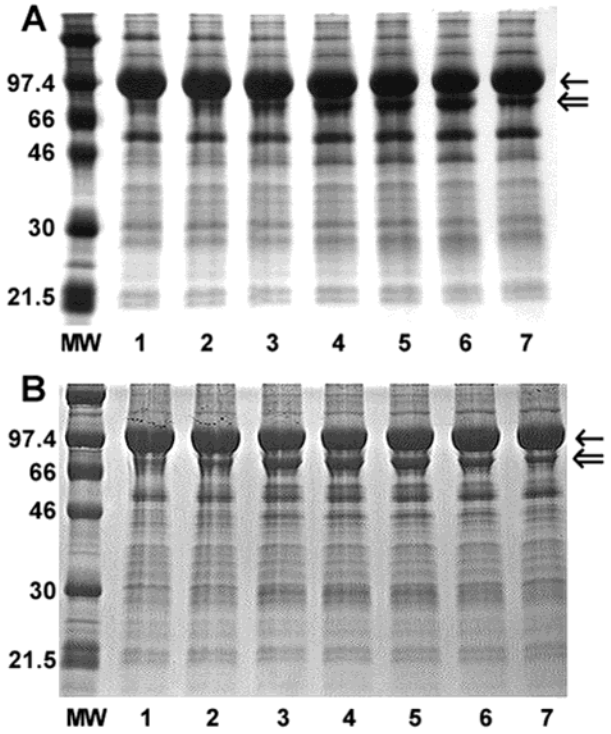

FIGURE 5: ATP or AMP-PNP concentration dependence of Fe^{2+}- and ascorbate-assisted ATPase cleavage. Incubation for 50 min, solubilization, and electrophoresis were performed as described under Methods. All samples were incubated in the presence of the following concentrations of ATP (A) or AMP-PNP (B): 1, none; 2, 10 μM; 3, 50 μM; 4, 0.1 mM; 5, 0.2 mM; 6, 0.5 mM; 7, 1.0 mM. The single arrow indicates the ATPase band, and the double arrow indicates cleavage products. The MW numbers refer to kDa.

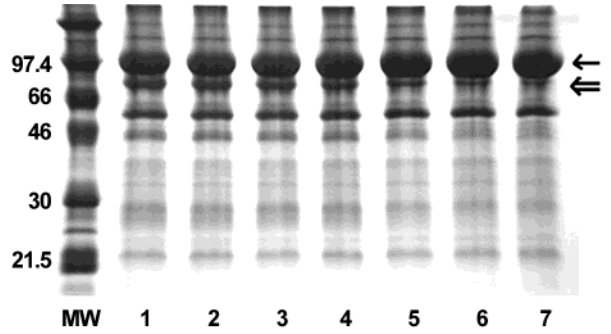

FIGURE 6: ATP-dependent, Fe^{2+}- and ascorbate-assisted cleavage is inhibited by Mg^{2+}. Incubation for 50 min, solubilization, and electrophoresis were performed as described under Methods. All samples were incubated in the presence of 0.2 mM AMP-PNP, but with different concentrations of $MgCl_2$: 1, 0; 2, 10 μM; 3, 50 μM; 4, 0.1 mM; 5, 0.5 mM; 6, 1.0 mM; 7, 5 mM. The single arrow indicates the ATPase band, and the double arrow indicates cleavage products. The MW numbers refer to kDa.

we reduced the protein with NaB^3H_4, following incubation with Fe^{2+} and ascorbate. H_2O_2 was not used in this case, as it would interfere with reduction by NaB^3H_4. The reduced protein was digested exhaustively with trypsin, and the soluble fragments were separated by HPLC. A single peptide was found to be radioactive, and was submitted to amino acid sequencing and determination of radioactive label. In these experiments, due to the clean trypsin cut, the analysis was unambiguous and the amino-terminal sequence was ^{437}VGEATETALTTLVEK^{451}, with most of the radioactive label on Thr441, and traces in the Glu442 peak (Figure 7). No incorporation of radioactivity was found when the

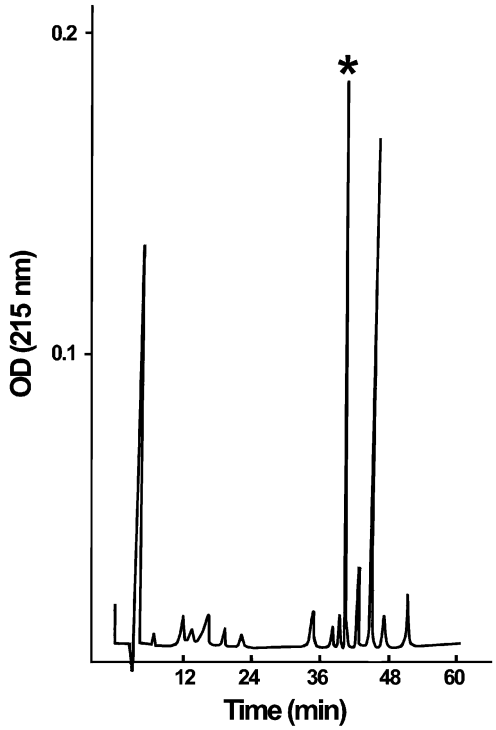

FIGURE 7: Purification and sequence of the ^{3}H-labeled peptide fragment. E1-Ca_2 samples were incubated with Fe^{2+} and ascorbate for 50 min as described under Methods, followed by reaction with NaB^3H_4, exhaustive trypsin digestion, and repeated HPLC separation. The graph in the figure represents the second separation, and the asterisk signifies the presence of radioactive ^{3}H-label in the eluted peptide.

incubation with Fe^{2+} and ascorbate was carried out in the absence of ATP or Ca^{2+} (i.e., E2-TG). Therefore, these experiments demonstrated a Ca^{2+}- and ATP-dependent oxidation of the Thr441 side chain, followed by very slow or no cleavage. It is noteworthy that oxidation of the Thr353 side chain by vanadate (near the catalytic Asp351) was previously demonstrated by the same technique (*16*).

DISCUSSION

We demonstrated that Fe^{2+}-catalyzed peptide bond cleavage near Ser346 and oxidation of the Thr441 side chain take place within SR Ca^{2+} ATPase. In the absence of H_2O_2, which accelerates the peptide bond cleavage at least 40×, the presence of ATP (or AMP-PNP) and Ca^{2+} was an absolute requirement. Because these reactions were inhibited by addition of Mg^{2+}, it is very likely that the locations identified here correspond to the Mg^{2+} binding sites. Then, a critical question is that how these sites are related to catalytically important Mg^{2+} and the substrate Mg^{2+}−ATP.

Cleavage at or near Ser346. Our experiments demonstrate that oxidative cleavage of the ATPase protein is produced very efficiently by Fe^{2+} with assistance of H_2O_2, and no requirement for ATP (Figure 2). The 70−75 kDa size of the carboxyl-terminal fragment, and the sequence analysis of its amino terminus, suggests that cleavage is produced by bound Fe^{2+} in proximity of Ser346. This residue resides in the P domain, near the L67 loop, and is surrounded by several oxygen atoms, including those of the Glu696 carboxyl group. Local interactions at this site are critical for correct protein folding and the occurrence of phosphorylation reactions (*18, 19*). In fact, mutation of Ser346 produces

catalytic inactivation (*18*). It is possible that this Fe^{2+} site corresponds to a Mg^{2+} site. It is known that Mg^{2+} binding is required for the reverse ATPase phosphorylation with P_i, in the absence of nucleotide (*20*).

Cleavage is not localized exclusively at Ser346, but involves neighboring residues to a significant extent. This pattern is likely related to diffusion of hydroxyl radicals formed in the presence of Fe^{2+}, and OH-dependent abstraction of hydrogen atoms from neighboring amino acid α-carbons (*9*), followed by peptide cleavage at multiple sites. The multiplicity of fragments (65−85 kDa size range) obtained when E2-TG was used (Figure 2) may reflect the difference in the diffusion pattern of hydroxy radicals or may reflect the different organization of the three cytoplasmic domains as proposed with Na^+, K^+ ATPase (*7*).

The ATP dependence of cleavage by Fe^{2+}, under conditions of limited assistance (i.e., in the presence of ascorbate), is puzzling, since cleavage at the same site is observed in the presence of H_2O_2 with no apparent requirement for ATP. The distance between Ser346 and the site (Asp351) of ATP γ-phosphate acceptance appears too large (approximately 16 Å) for a direct role of the Fe^{2+}−ATP complex bound to the substrate site. It is conceivable that the binding of ATP places the Ca^{2+} ATPase into a certain conformation (*21*) in which the binding of Fe^{2+} is facilitated, and that the frequency of taking such a conformation is very limited in the absence of ATP. Presumably, facilitation by ATP is not required under conditions producing large quantities of hydroxyl radicals, such as in the presence of H_2O_2.

Oxidation of Thr441. An interesting finding is related to the Ca^{2+}- and ATP-dependent oxidation of Thr441 by Fe^{2+}, because this provides the first direct evidence on the location of Mg^{2+} and, accordingly, the γ-phosphate of Mg^{2+}-ATP in $E1\text{-}Ca_2$. Oxidation is tightly localized to this residue, and is not followed by detectable peptide cleavage. It should be pointed out that detection of the oxidation product is based on reduction with NaB^3H_4, which is a reaction well characterized for the aldehyde product of threonine side chain oxidation (*10*). A rather complex and relatively slow pathway for peptide cleavage, following oxidation of the threonine side chain, explains the relatively high steady-state level of oxidized intermediate.

Thr441 resides within the N-domain of the SR ATPase, and the requirement for ATP is consistent with involvement of the bound Fe^{2+}−ATP complex in the oxidation reaction. The location of the bound Fe^{2+}−ATP complex is likely to correspond to that of the Mg^{2+}−ATP complex, when Mg^{2+} is present instead of Fe^{2+} under conditions of catalytic activation. A similar position for Mg^{2+} was proposed by Patchornik et al. (*7*) for Na^+, K^+ ATPase, although they observed several cleavage products due to the usage of H_2O_2 in addition to ascorbate.

To evaluate its proximity to pertinent residues, we modeled the bound Mg^{2+}−ATP complex according to the location of ADP in the crystal structure of Ca^{2+} ATPase in the E2-TG form (Figure 8; *2*). We took advantage of the fact that ADP (present during crystallization) was detectable in these crystals, even though its electron density was rather low presumably due to the low affinity of the E2-TG form for ADP. We then considered the Mg^{2+}−ATP conformation derived from high-resolution structures of other enzymes, as well as by NMR studies (*22*), and fitted the β-phosphate

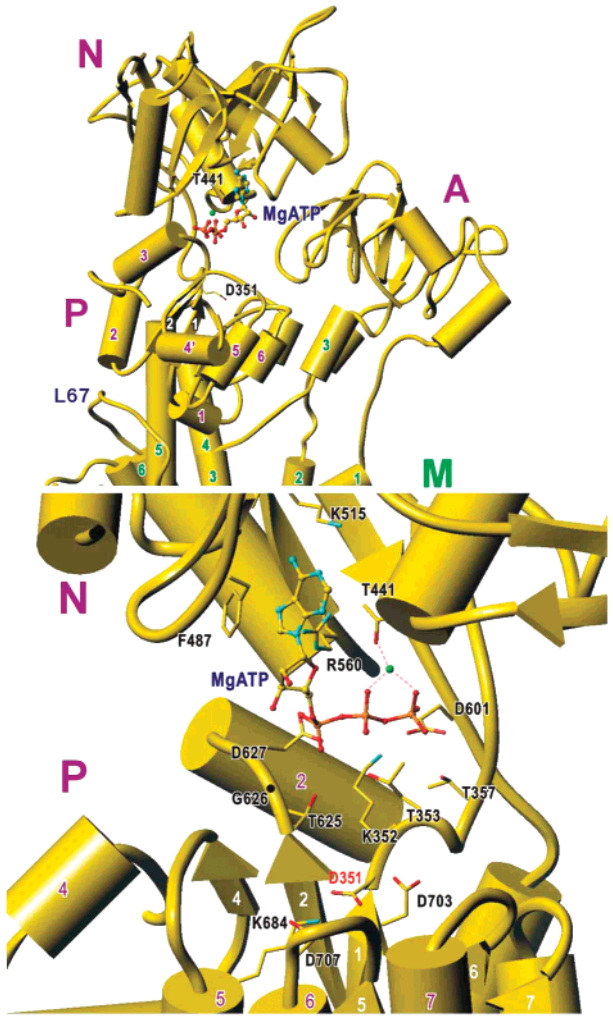

FIGURE 8: Modeling of the Mg−ATP complex within the ATPase structure. Top: Mg^{2+}−ATP in Ca^{2+} ATPase as deduced from the crystal structure of Ca^{2+} ATPase in the E_2-TG state (*2*) and oxidation with Fe^{2+}−ATP. Mg^{2+}−ATP is in ball-and-stick. Helices appear as cylinders and the strands as arrows. The side chain for the phosphorylation residue, Asp351, in the P-domain is also shown. The P4 helix in the P-domain is removed. When 2 Ca^{2+} bind, the N-domain will approach closer to the P-domain, whereas the A-domain will be detached to allow approach of the N-domain. Bottom: a close-up of the structure around Mg^{2+}−ATP at the N−P interface. The direction of the movement of the N-domain is approximately normal to the plane of the paper. Side chains are shown for some of the critical residues. Dotted lines connect the Mg^{2+} (central sphere) and oxygen atoms within a 2.5 Å distance.

of the Mg^{2+}−ATP complex to that of ADP in our E2-TG crystal. Without any manual adjustment, the Mg^{2+} of the Mg^{2+}−ATP complex fell very close to the side chain oxygen of Thr441, at a distance of approximately 2.3 Å when any of four Mg^{2+}−ATP structures obtained from the PDB (1KAX, 1A82, 1F2U, 1MJH) was used. The next closest oxygen atom is that of Glu442, which is much less oxidized but detectable. The ATP adenosine moiety of the fitted Mg^{2+}−ATP complex resides in a pocket delimited by Lys492 and Lys515 in the N domain, with stabilization provided by the neighboring Arg560. ATP takes a folded conformation, and Mg^{2+} is stabilized by the phosphate oxygen atoms, as well as by the Thr441 side chain in close proximity; the β-phosphate is stabilized by Thr353 in the P-domain, and the γ-phosphate comes very close to Asn359 and Asp601 in the hinge region (Figure 8). Such a structural representa-

tion is in very good agreement with the experimental finding of Thr441 oxidation by the Fe^{2+}−ATP complex.

It should be pointed out, however, that in this arrangement of the cytoplasmic domains in E2-TG state (Figure 8), the ATP-terminal phosphate is not sufficiently close to the P-domain to allow phosphoryl transfer to Asp351. Even though in the E1-Ca_2-ATP state the N-domain may approach further the P-domain, the γ-phosphate of ATP would not be able to reach Asp351 with this folded conformation of ATP. On the other hand, a better approximation (not shown) is obtained if Mg^{2+}−ATP takes more common extended conformations by changing its torsion angles between the α- and β-phosphates. It is possible that, following binding to E1-Ca2 in solution, the Mg^{2+}−ATP complex undergoes fluctuations permitting γ-phosphate approximation to Asp351. Or, there may be an integrated mechanism to change the conformation of ATP when the N-domain approaches the P-domain. For example, the γ-phosphate in the E2-TG model comes actually too close to Asp601 and Asn359 in the hinge region. It is possible that the configuration of the cytoplasmic domains, following stabilization by the binding of Mg^{2+}−ATP, is slightly more opened than in the E2-TG structure shown in Figure 8. A more favorable interfacing of the N-domain to the P-domain would then reorient the γ-phosphate of ATP to the right direction by interaction of the residues in the hinge region. Assuming such changes in Mg^{2+}−ATP, detection of Thr441 side chain oxidation in our experiments is due to approximation (even with low frequency) of the folded Fe^{2+}−ATP complex to this residue.

With respect to global conformational states of the enzyme, it is interesting that an experimental finding obtained in the presence of Ca^{2+} (open conformation) could be modeled satisfactorily using the E2-TG closed conformation. This is most likely due to the initial requirement of the open conformation for nucleotide binding, which in turn induces the closed conformation as required by the catalytic mechanism.

REFERENCES

1. Toyoshima, C., Nakasako, M., Nomura, H., and Ogawa, H. (2000) Crystal structure of the calcium pump of sarcoplasmic reticulum at 2.6 Å resolution. *Nature 405*, 647−655.
2. Toyoshima, C., and Nomura, H. (2002) Structural changes in the calcium pump accompanying the dissociation of calcium. *Nature 418*, 605−611.
3. Toyoshima, C., Sasabe, H., and Stokes, D. L. (1993) Three-dimensional cryo-electron microscopy of the calcium ion pump in the sarcoplasmic reticulum membrane. *Nature 362*, 469−471.
4. Zhang, P., Toyoshima, C., Yonekura, K., and Stokes, D. L. (1998) Structure of the calcium pump from sarcoplasmic reticulum at 8-Å resolution. *Nature 392*, 835−839.
5. Degani, C., and Boyer, P. D. (1973) A borohydride reduction method for characterization of the acyl phosphate linkage in proteins and its application to sarcoplasmic reticulum adenosine triphosphatase. *J. Biol. Chem. 248*, 8222−8226.
6. Bastide, F., Meissner, G., Fleischer, S., and Post, R. L. (1973) Similarity of the active site of phosphorylation of the ATPase for transport of sodium and potassium ions in kidney to that for transport of calcium ion in sarcoplasmic reticulum of muscle. *J. Biol. Chem. 248*, 8385−8391.
7. Patchornik, G., Goldshleger, R., and Karlish, J. D. (2000) The complex ATP−Fe^{2+} serves as a specific affinity cleavage reagent in ATP−Mg^{2+} sites of Na, K-ATPase: Altered ligation of Fe^{2+} (Mg^{2+}) ions accompanies the $E_1P \rightarrow E_2P$ conformational change. *Proc. Natl. Acad. Sci. U.S.A. 97*, 11954−11959.
8. Platis, I. E., Ermacora, M. R., and Fox, R. O. (1993) Oxidative polypeptide cleavage mediated by EDTA-Fe covalently linked to cysteine residues. *Biochemistry 32*, 12761−12767.
9. Berlett, B. S., and Stadtman, E. R. (1997) Protein oxidation in aging, disease, and oxidative stress. *J. Biol. Chem. 272*, 20313−20316.
10. Grammer, J. C., Loo, J. A., Edmonds, C. G., Cremo, C. R., and Yount, R. G. (1996) Chemistry and mechanism of vanadate-promoted photooxidative cleavage of myosin. *Biochemistry 35*, 15582−15592.
11. Eletr, S., and Inesi, G. (1972) Phospholipid orientation in sarcoplasmic reticulum membranes: Spin label and proton NMR studies. *Biochim. Biophys. Acta 282*, 174−179.
12. Sagara, Y., Wade, J. B., and Inesi, G. (1992) A conformational mechanism for formation of a dead-end complex by the sarcoplasmic reticulum ATPase with thapsigargin. *J. Biol. Chem. 267*, 1286−1292.
13. Hua, S., Ma, H., Lewis, D., Inesi, G., and Toyoshima, C. (2002) Functional role of "N" (nucleotide) and "P" (phosphorylation) domain interactions in the sarcoplasmic reticulum (SERCA) ATPase. *Biochemistry 41*, 2264−2272.
14. Lanzetta, P. A., Alvarez, L. J., Reinsch, P. S., and Candia, O. A. (1979) An improved assay for nanomole amounts of inorganic phosphate. *Anal. Biochem. 100*, 95−97.
15. Laemmli, U. K. (1970) Cleavage of structural proteins during the assembly of the head of bacteriophage T4. *Nature 227*, 680−685.
16. Hua, S., Inesi, G., and Toyoshima, C. (2000) Distinct topologies of mono- and decavanadate binding and photooxidative cleavage in the sarcoplasmic reticulum Ca^{2+}-ATPase. *J. Biol. Chem. 275*, 30546−30550.
17. Clarke, D. M., Loo, T. W., Inesi, G., and MacLennan, D. H. (1989) Location of high affinity Ca^{2+}-binding sites within the predicted transmembrane domain of the sarcoplasmic reticulum Ca^{2+}-ATPase. *Nature 339*, 476−478.
18. Zhang, Z., Lewis, D., Sumbilla, C., Inesi, G., and Toyoshima, C. (2001) The role of the M6-M7 loop (L67) in stabilization of the phosphorylation and Ca^{2+} binding domains of the sarcoplasmic reticulum Ca^{2+}-ATPase (SERCA). *J. Biol. Chem. 276*, 15232−15239.
19. Sorensen, T., and Andersen, J. P. (2000) Importance of stalk segment S5 for intramolecular communication in the sarcoplasmic reticulum Ca^{2+}-ATPase. *J. Biol. Chem. 275*, 28954−28961.
20. Masuda, H., and deMeis, L. (1973) Phosphorylation of the sarcoplasmic reticulum membrane by orthophosphate. Inhibition by calcium ions. *Biochemistry 12*, 4581−4585.
21. Danko, S., Yamasaki, K., Daiho, T., Suzuki, H., and Toyoshima, C. (2001) Organization of cytoplasmic domains of sarcoplasmic reticulum Ca^{2+}-ATPase in E_1P and E_1ATP states: a limited proteolysis study. *FEBS Lett. 505*, 129−135.
22. Klevickis, C., and Grisham, C. M. (1982) Phosphorus-31 nuclear magnetic resonance studies of the conformation of an adenosine 5′-triphosphate analogue at the active site of ($Na^+ + K^+$)-ATPase from kidney medulla. *Biochemistry 21*, 6979−6984.

BI026181U